Progress In Electromagnetics Research C, Vol. 95, 47–57, 2019

A Novel Microstrip Fed L-Shaped Arm Slot and Notch Loaded RMPA with Mended Ground Plane for Bandwidth Improvement

Mukesh Kumar*, Jamshed A. Ansari, Abhishek K. Saroj, Rohini Saxena, and Devesh

Abstract—In this paper a novel design of microstrip fed L-shaped arm slot and notch loaded RMPA (Rectangular Microstrip Patch Antenna) with mended ground plane for wide bandwidth is presented. The proposed prototype antenna is fabricated on an FR-4 (Fire retardant) substrate with dimension $30 \times 30.8\,\text{mm}^2$ and 1.6 mm thickness. The proposed design is analyzed and simulated using high frequency structure simulator (HFSS) tool version 15. The analysed results are validated through fabrication and measurement results. The analyzed result shows 96.1% maximum radiation efficiency at 2.9 GHz whereas overall efficiency is more than 85% over the entire frequency range, and experiment achieves gain 8.4 dB at 7 GHz. The designed antenna achieves 119.39% impedance bandwidth with more than 5 dB gain over the operating frequency range of 2.41 GHz to 9.55 GHz. For better performance and analysis of proposed antenna, a parametric study has been carried out to analyze the effects of variations in the following-slot and notch dimensions loaded on the patch as well as variations in ground length. The designed antenna can be utilized for various applications incorporating Bluetooth, WLAN, Wi-Max, and UWB operation.

1. INTRODUCTION

Microstrip Patch Antennas (MPAs) have prominent position in modern wireless communication technology or ultra-wide band (UWB) applications because of their salient attributes like thin profile, light weight, low cost and can be mounted to any host surfaces. MPA also suffers from some limitations such as constricted bandwidth, lower gain, and poor efficiency [1, 2]. Several designs and techniques of MPAs are investigated for enhancing impedance bandwidth such as different types of feedline, slots and notches in radiator, through stacking and multilayer structures by the researchers and scientists in past several decades [3, 4]. In last few years, monopole microstrip patch antennas with defected ground structure (DGS) become more popular to overcome these limitations due to their facile geometry. Microstrip fed monopole antennas are presented for bandwidth expansion using bevel technique [5, 6] and double U-slot loaded DGS trapezoid patch monopole antenna with very large dimension [7]. In [8], a (CPW) coplanar waveguide fed $34\times34\,\text{mm}^2$ monopole MPA has been demonstrated for UWB application with a low loss dielectric substrate. Several designs of patch antennas with mended ground plane are also presented for large operated bandwidth [9–14]. Some papers are reported in the literature where various techniques are used to achieve better radiation pattern, UWB, and current distribution over the radiating elements such as a coplanar wave guide fed monopole antenna using defected substrate [15], rhombus strip bounded annular ring antenna derived by microstrip feedline using DGS [16], compact U shaped modified circular ground plane antenna [17], curved slot loaded rectangular patch monopole MPA [18], microstrip fed monopole antenna by using beveled technique in ground plane [19], round steps on the corner loaded rectangular MPA [20], a modified rectangular patch monopole MPA [21], symmetrical hexagonal radiator monopole antenna [24], asymmetrical U-shaped patch loaded with

Received 20 May 2019, Accepted 1 August 2019, Scheduled 25 August 2019
* Corresponding author: Mukesh Kumar (mukesh044@gmail.com).
The authors are with the University of Allahabad, India.

T-shaped strip monopole antenna [25], circularly polarized MPA with different feeds and radiating shapes [23, 27, 28] for bandwidth expansion. Additionally, the impacts of metallic and dielectric wedges are explored to improve radiation attributes [29–31]. They have also derived an expression for physical instinct about the utilization and function of anisotropy parameters, which cover a variety of inverse problems of practical interest existing inside an electromagnetics laboratory such as parts of waveguides, antennas, and reflectors.

The aim of proposed design is based on a monopole antenna structure and above mentioned literature to study how to overcome the limitation of narrow bandwidth and achieve better gain. In this paper, a pair of L-shape arm slots and a notch loaded RMPA are studied and analyzed. The proposed antenna is derived from a microstrip feedline by selecting proper positions and dimensions of slots and notches on the radiator with finite ground plane for improving the bandwidth (BW) and gain. A parametric variation is also studied for geometrical extension. The simulated and experimented results agree well. A brief comparison is reported in Table 1 between the proposed and some previously designed monopole antennas. The proposed design is compared with different designs in which substrates and feeding mechanisms are same. The proposed design shows 119.39% bandwidth, 96% efficiency, and more than 8 dB gain which show better results from the compared references. But [26] presents better bandwidth and low gain in comparison to the proposed design.

Table 1. Comparison with previously designed monopole type antennas.

Ref.	**Dimensions (mm^3)**	**Bandwidth (%)**	**Maximum Gain (dB)**	**Efficiency (%)**	**Feeding Method**	**Applications**	**Substrate**
Ref. [15]	$36 \times 42 \times 1.6$	100%	6.08	88	CPW	C and X band	FR-4
Ref. [16]	$25 \times 38 \times 1.6$	86.71	2.85	Not Given	Microstrip Line	WLAN/WiMAX	FR-4
Ref. [18]	$50 \times 55 \times 1.5$	109	4.8	Not Given	Microstrip Line	WLAN/WiMAX	FR-4
Ref. [19]	$30 \times 28 \times 0.8$	112	3.76	98	Microstrip Line	UWB	FR-4
Ref. [20]	$30 \times 35 \times 1.6$	109.5	6	Not Given	Microstrip Line	UWB	FR-4
Ref. [21]	$20 \times 25 \times 1.5$	110.79	5.1	89	Microstrip Line	UWB	FR-4
Ref. [23]	$49 \times 55 \times 1.5$	106.3	5.11/less than 8	Not Given	Microstrip Line	wireless communication systems	FR-4
Ref. [24]	$20 \times 25 \times 1.6$	118.8	5.1	Not Given	Microstrip Line	short band radio wave communications,	FR-4
Ref. [25]	$34 \times 20 \times 1.6$	107.35	4.91	70	Microstrip Line	Bluetooth, WLAN, Wi-Max etc.	FR-4
Ref. [26]	$52.25 \times 42 \times 1.575$	167.22	Less than 4.5	Not Given	Microstrip Line	LTE2600, Wi-Fi, WLAN and UWB	Rogers RT duroid 5880
Proposed	$30 \times 30.8 \times 1.6$	119.39	8.44	96.1	Microstrip Line	Bluetooth, WLAN, Wi-Max, S and C band	FR-4

2. ANTENNA GEOMETRICAL CONFIGURATIONS

The designed antenna is fabricated on an FR-4 substrate with dielectric constant $\varepsilon_r = 4.4$ and loss tangent $\tan\delta = 0.02$. The optimized length and width of patch are 18.64 mm and 28.12 mm with 1.6 mm substrate height. The dimension of substrate and length of ground conductor is considered as $30 \times 30.8\,\text{mm}^2$ and 9.8 mm, respectively. For proper impedance matching, a 50 Ω microstrip line is used to energize the patch. The configured geometry of designed antenna is shown in Figure 1.

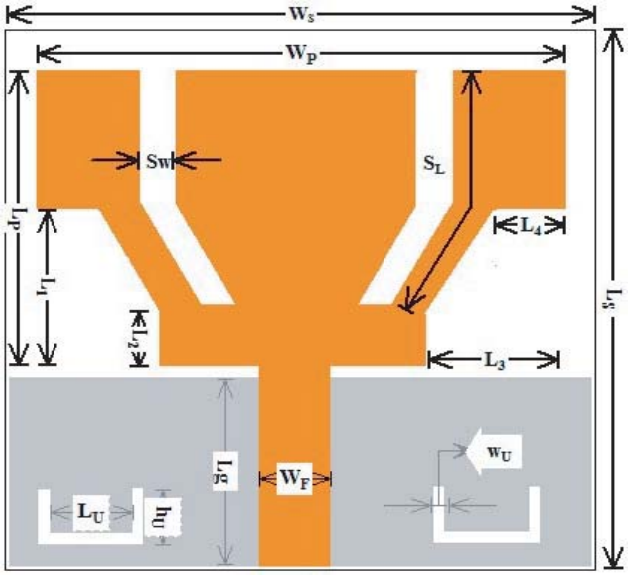

Figure 1. Proposed antenna design configuration.

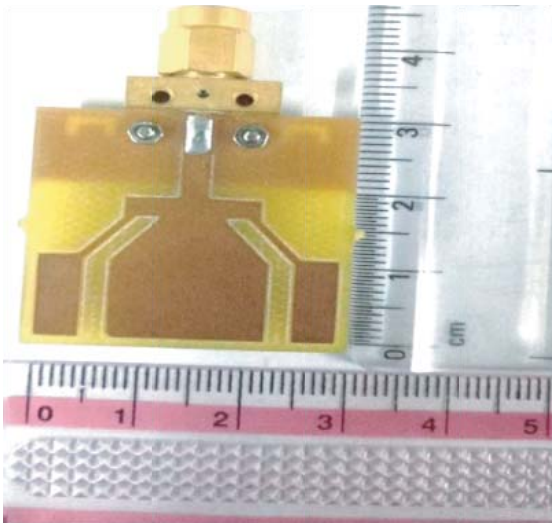

Figure 2. Dimensions of fabricated antenna.

The structure of the designed antenna is tuned on the basis of optimization, and the work is carried out by using Ansoft's High Frequency Structure Simulator (HFSS) tool. The details of geometrical specifications of fabricated antenna are provided in Table 2. The fabricated model of designed antenna is demonstrated in Figure 2.

Table 2. Optimized geometrical specifications of proposed antenna.

Parameter	$\mathbf{W_S}$	$\mathbf{L_S}$	$\mathbf{W_P}$	$\mathbf{L_P}$	**Sw**	$\mathbf{S_L}$	$\mathbf{W_F}$	**Lg**
Dimension (mm)	30	30.8	28.12	18.64	1.87	15.82	3	9.8
Parameter	$\mathbf{L_U}$	$\mathbf{h_U}$	$\mathbf{W_U}$	**h**	**L1**	**L2**	**L3**	**L4**
Dimension (mm)	3	2	0.5	1.6	7.5	2.81	7.5	3.75

3. ANTENNA DESIGN PROCEDURE AND PERFORMANCES

Development of the proposed antenna has been introduced in four steps as demonstrated in Figure 3, and its performance in terms of simulated reflection coefficient (S_{11}) is indicated in Figure 4. In the first step, single band (3.20–4.42 GHz) with 32.02% of impedance bandwidth is obtained, when an RMPA with symmetrical equilateral arm U-slots loaded on a finite ground conductor is considered. In the second step, when symmetrical I-slots are included in the planar patch for excitation of lower order resonances, dual bands (3.1–3.85 GHz and 3.91–4.52 GHz) are found with 21.58% and 14.47% of impedance bandwidths. In the third step, symmetrical tilted L-slots are loaded in patch section,

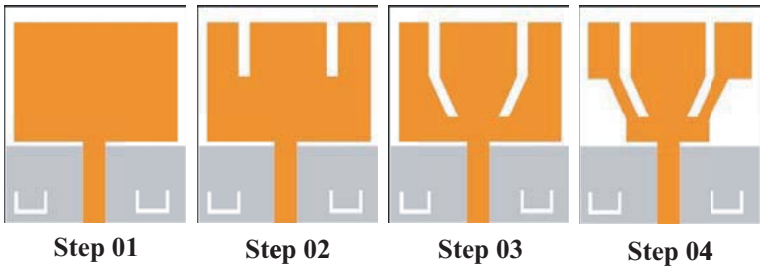

Figure 3. Development of antenna design steps.

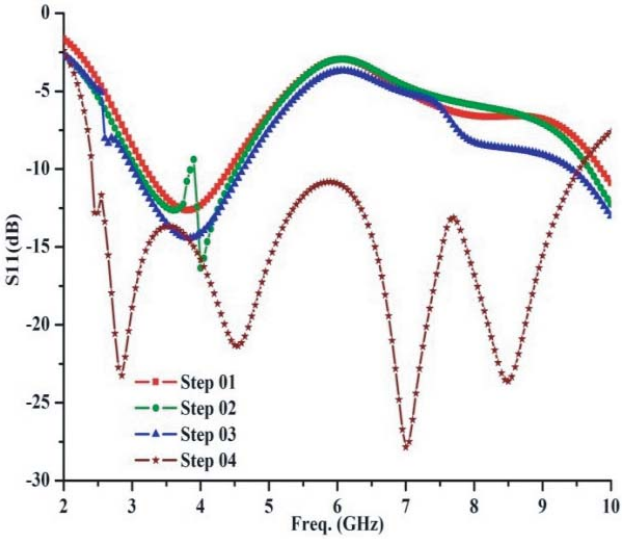

Figure 4. Simulated reflection coefficient of different iterations.

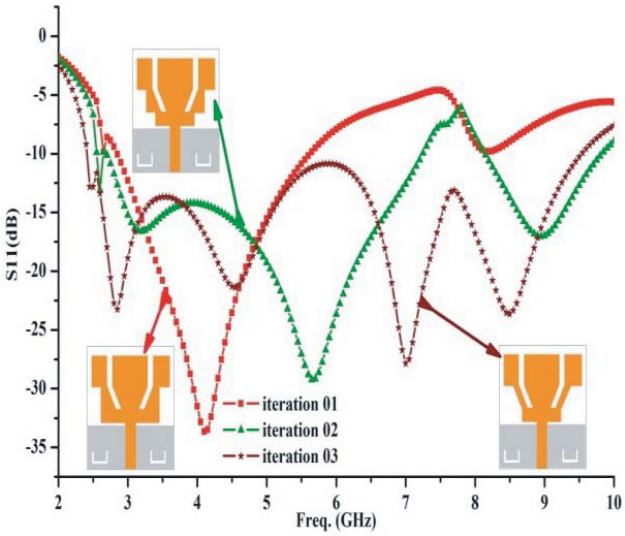

Figure 5. Simulated reflection coefficient of different steps.

which helps to shift the frequency in the lower operating band (3–4.62 GHz) with 42.51% impedance bandwidth. Better impedance matching is achieved with lower order resonance, when symmetrical notches are added in the patch section in the next step. It provides 119.397% bandwidth over the frequency range of 2.41–9.55 GHz, which is the final step of the proposed antenna.

For the final step, 03 iterations are considered with the performance in terms of reflection coefficient which is indicated in Figure 5. In the 1st iteration, when the symmetrical single step notch is added in the third step, the frequency is shifted in lower operating band (2.85–5.6 GHz) with 65.08% impedance bandwidth.

In the 2nd iteration, when double step notches are added, the dual bands are obtained at 2.7–7.2 GHz and 8.15–9.8 GHz with 90.9% and 18.38% of impedance bandwidth. In the 3rd iteration, the large operating band at 2.41–9.55 GHz with 119.39% impedance bandwidth is achieved, which is the final iteration of the designed antenna.

3.1. Parametric Study of Proposed Antenna

The impacts of various parameters are studied and investigated, which are accountable for antenna characteristics. Figure 6 shows the variation of simulated reflection coefficient with different parameters such as ground length (Lg), slot width (Sw), $L1$ (length of notch side 1), $L2$ (length of notch side 2), $L3$ (width of notch side 1), and $L4$ (width of notch side 2).

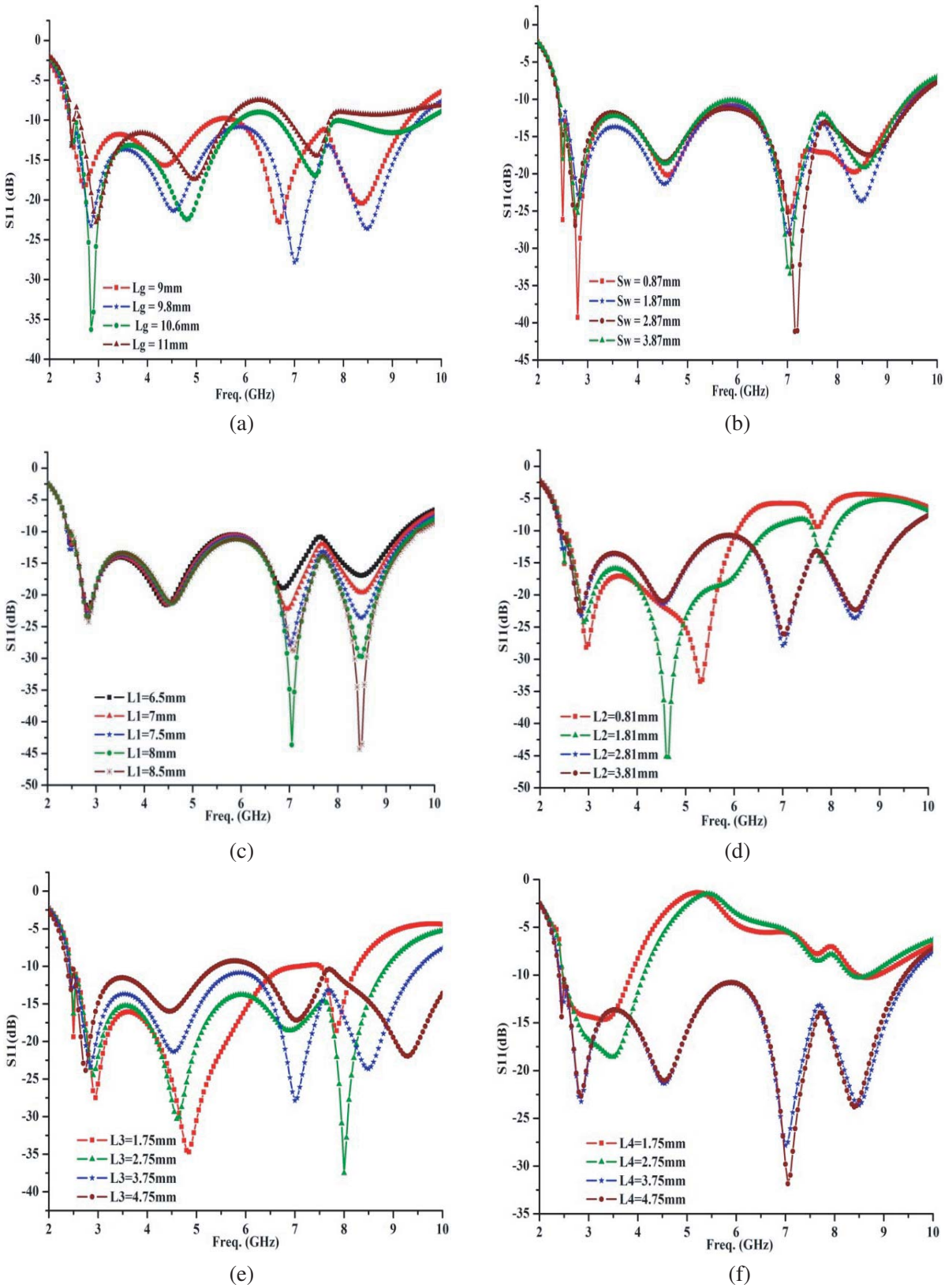

Figure 6. Simulated reflection coefficient variation for (a) Lg, (b) Sw, (c) $L1$, (d) $L2$, (e) $L3$ and (f) $L4$.

3.1.1. Effects of Ground Length (Lg)

The impact of reflection coefficient for different estimations of ground length (Lg) with other fixed optimized parameters is introduced in Figure 6(a). Ground length is shifted from 9 mm to 11 mm with 0.4 mm interim, and at the ideal estimation of 9.8 mm, we accomplish better impedance matching which provide improved bandwidth. Further variations in ground length degrade both impedance matching and bandwidth.

3.1.2. Effects of Slot Width (Sw)

Examining the variation of slot width (Sw) is carried out with other fixed optimized parameters. Figure 6(b) demonstrates the relating reflection coefficient. Slot width is varied from 0.87 mm to 3.87 mm with an interval of 1 mm. The impedance matching and bandwidth are slightly varied with slot width. The overall bandwidth achieves 6.95 GHz, 7.14 GHz, 7.05 GHz, and 6.9 GHz for the slot widths 0.87 mm, 1.87 mm, 2.87 mm, and 3.87 mm, respectively. At optimum value of 1.87 mm, improved bandwidth is achieved.

3.1.3. Effects of L1

Figure 6(c) indicates the impact of reflection coefficient for different values of $L1$. The volumes of other optimized elements are fixed. The length of "$L1$" is changed from 6.5 mm to 8.5 mm with an interval of 0.5 mm. The overall impedance bandwidth is slightly increased (6.9 GHz, 6.95 GHz, and 7.14 GHz) as "$L1$" is increased from 6.5 mm to 7.5 mm. When "$L1$" is extended from 7.5 mm to 8.5 mm, the frequency band is slightly shifted towards higher order resonance with 7.05 GHz impedance bandwidth. The maximum bandwidth is obtained at $L1 = 7.5$ mm.

3.1.4. Effects of L2

The variation of reflection coefficient for different estimations of $L2$ with other fixed streamlined parameters is discussed in Figure 6(d). When the length of "$L2$" is shifted from 0.81 mm to 3.81 mm with 1 mm gap, various frequency bands are observed. At the length of "$L2 = 0.81$ mm", antenna radiates just over the frequency scope of 2.45 to 6.05 GHz. It is found that the antenna shows dual frequency bands from 2.45 to 6.7 GHz and 7.65 to 8.05 GHz, if the range of "$L2$" is increased by 1 mm. As the range of "$L2$" is further increased from 1.81 mm to 2.81 mm and 2.81 mm to 3.81 mm, the frequency band is obtained at 2.41 to 9.55 GHz and 2.45 to 9.5 GHz. At the ideal estimation of "$L2 = 2.81$ mm", a superior impedance matching is accomplished.

3.1.5. Effects of L3

Figure 6(e) exhibits the impact of reflection coefficient on the antenna execution for different estimations of $L3$. The components of other optimized parameters are considered fixed. When the range of "$L3$" is differed from 1.75 mm to 4.75 mm with the interval of 1 mm, various frequency bands are obtained at 2.45 to 8.25 GHz, 2.45 to 8.85 GHz, 2.41 to 9.55 GHz, as well as 2.4 to 5.35 GHz and 6.2 to 10 GHz. At the optimum width of "$L3 = 3.75$ mm", a better impedance matching is achieved.

3.1.6. Effects of L4

The impact of reflection coefficient for different widths of $L4$ with other optimized parameters is demonstrated in Figure 6(f). Different frequency bands are obtained, when the range of "$L4$" is differed from 1.75 mm to 4.75 mm. The dual frequency behaviour is found at 2.5–3.85 GHz and 8.5–8.85 GHz, 2.5–4.1 GHz, and 8.35–8.65 GHz for "$L4 = 1.75$ mm and 2.75 mm". As the value of "$L4$" is further increased (from 2.75 to 4.75 mm), it is seen that the estimation of "$L4 = 3.75$ mm" offers superior impedance matching.

From Figure 6, parametric variations of different dimensions of the proposed antenna are studied and observed, and the gap between radiation patch and ground plane length (Lg) plays an important role for obtaining wide band features. The length of the ground plane controls the coupling between the

ground and the patch. It acts as an additional impedance matching network. The gap size influences the impedance matching, and hence placing symmetrical notches ($L1$, $L2$, $L3$, and $L4$) at the bottom of the patch, results in smooth transition from one resonant mode to another resonant mode and ensuring good impedance match over a operating frequency range 2.41 to 9.55 GHz.

4. RESULTS AND DISCUSSIONS

The proposed antenna is fabricated on an FR-4 substrate using a CNC machine, and measurement is carried out using Agilent Vector Network Analyzer E5071C. Figure 7(a) demonstrates the correlation of simulated and measured reflection coefficients of the proposed antenna. The simulated and measured results are slightly shifted due to fabrication tolerances and software limitations in terms of modelling and simulating over a large bandwidth. Figure 7(b) exhibits the comparison of simulated and measured voltage standing wave ratios (VSWRs) of the proposed antenna. For the entire frequency range of simulation and measurement at 2.41–9.55 GHz and 2.70–10 GHz, VSWR is maintained with less than two (VSWR $\leq$ 2). There is a good correlation between measured and simulated results. Figure 7(c) shows the comparison of simulated and measured gains of the proposed antenna. Gain is measured by two antenna method [22] by using horn antenna and proposed prototype antenna in an anechoic

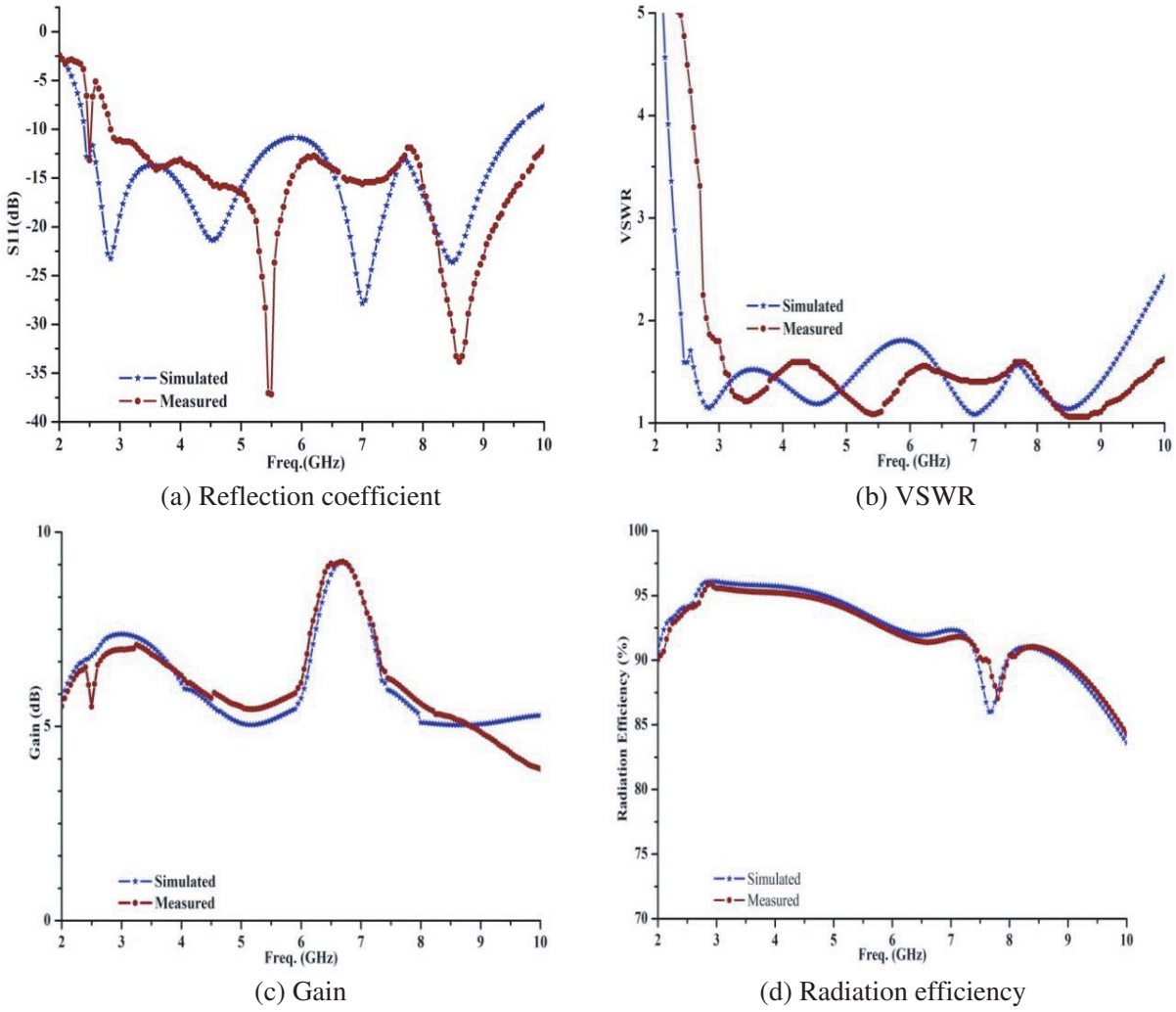

(a) Reflection coefficient

(b) VSWR

(c) Gain

(d) Radiation efficiency

Figure 7. Comparison of simulated and measured results of the proposed antenna for (a) S_{11}, (b) VSWR, (c) gain, (d) radiation efficiency.

chamber. The maximum measured gain of 8 dB at 7 GHz is achieved. Figure 7(d) shows the comparison of simulated and measured radiation efficiencies (%) of the proposed antenna. More than 85% radiation efficiency is achieved for the entire operating band.

At higher frequencies, dielectric loss increases which causes reduction in radiation efficiency. Figures 8(a) and (b) show the measured results of reflection coefficient and VSWR on VNA. VNA and anechoic chamber setup for the proposed antenna are shown in Figures 8(c) and (d).

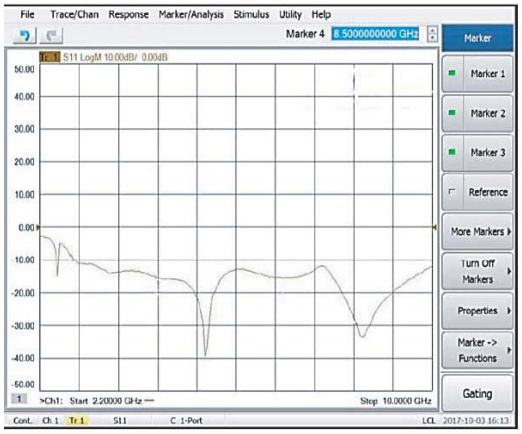

(a) Reflection coefficient

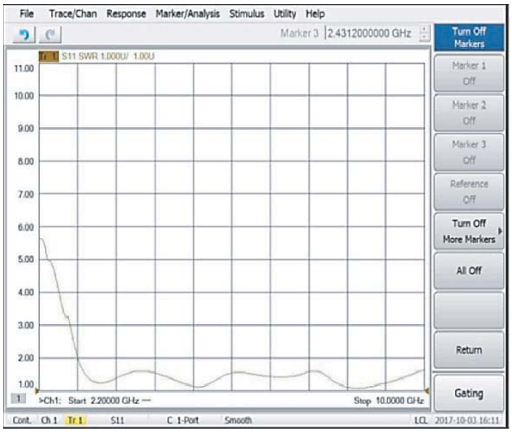

(b) VSWR

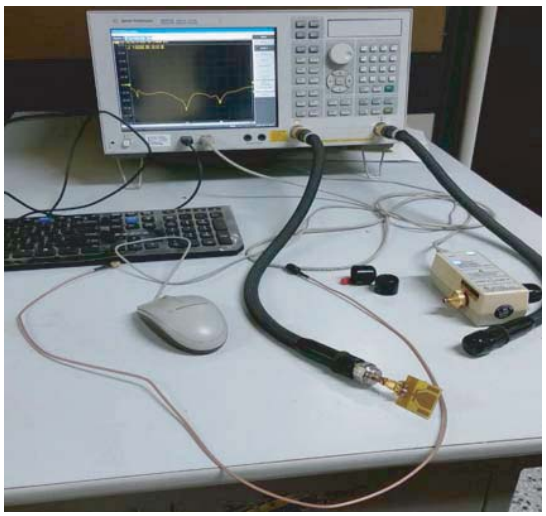

(c) VNA setup

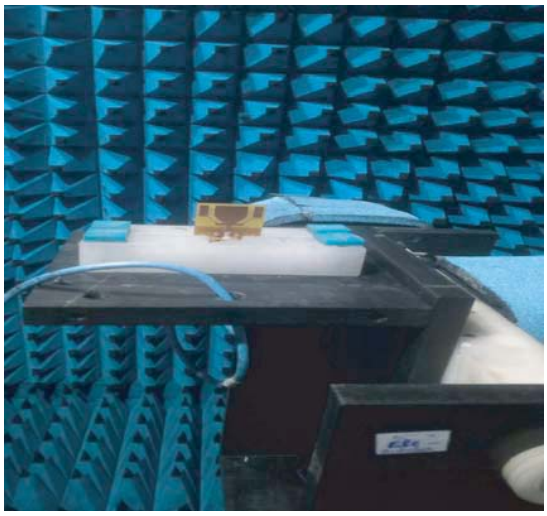

(d) Antenna snap in anechoic chamber

Figure 8. (a) Measured reflection coefficient, (b) measured VSWR on VNA, (c) VNA setup and (d) antenna snap in anechoic chamber.

Figures 9(a), (b), (c), and (d) show the simulated 2D radiation patterns of the proposed antenna, and the co-polarization and cross polarization for E-plane and H-plane at resonating frequencies of 2.85 GHz, 4.55 GHz, 7 GHz, and 8.5 GHz are shown, respectively. The maximum cross-polarization level is -19.8 dB and -41.4 dB, -17.3 dB and -41.7 dB, -20.6 dB and -35.8 dB as well as -20 dB and -35.1 dB at 2.85 GHz, 4.55 GHz, 7 GHz, and 8.5 GHz respectively for E-plane and H-plane. The cross-polarization values are 17–20 dB and 35–42 dB lower than the co-polarized values for E-plane and H-plane, respectively.

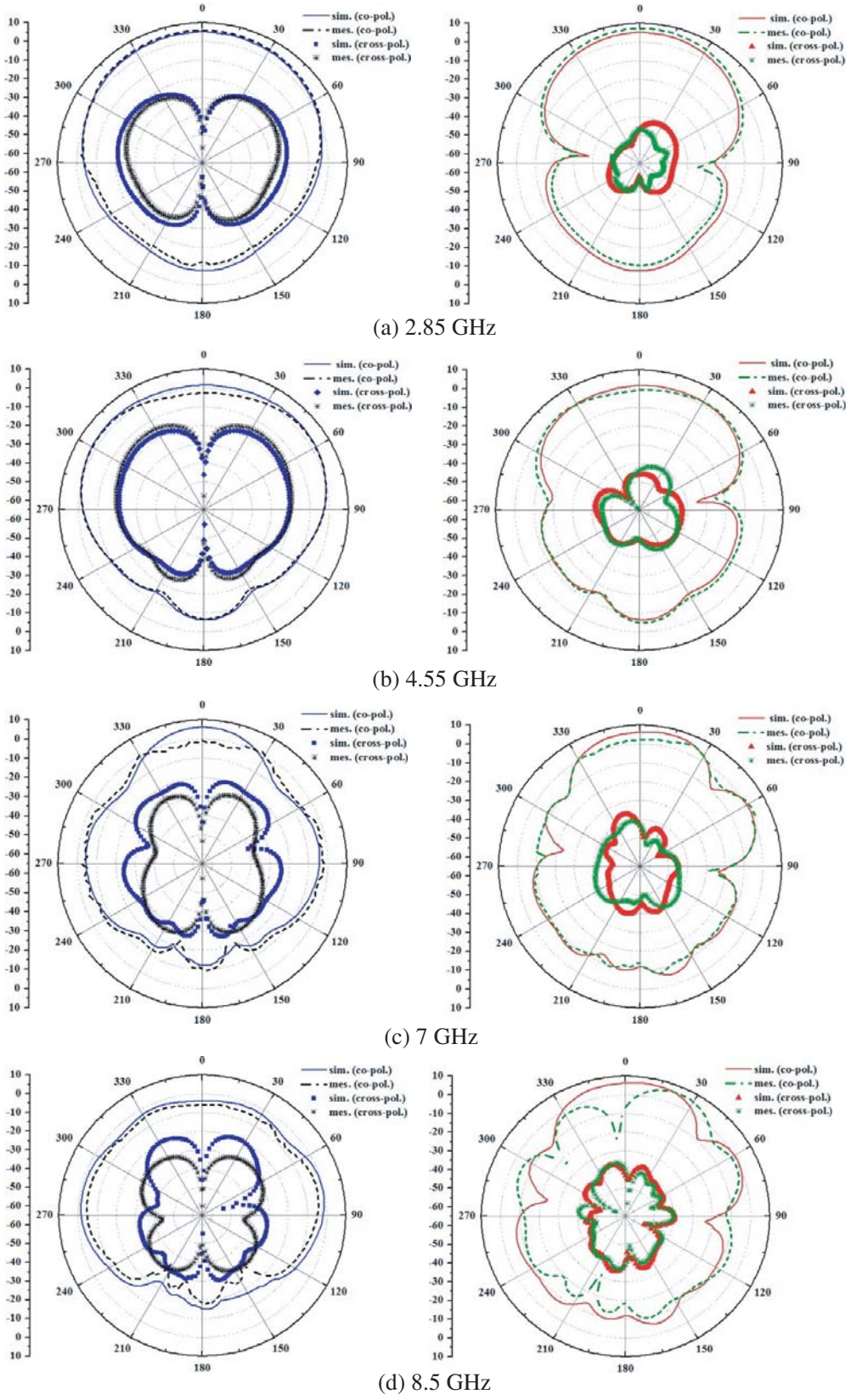

Figure 9. Simulated radiation pattern of proposed antenna at different resonant frequencies (Left side shows E-plane and right side H-plane). (a) 2.85 GHz, (b) 4.55 GHz, (c) 7 GHz and (d) 8.5 GHz.

5. CONCLUSION

A compact microstrip fed L-shaped arm slot and notch loaded RMPA (Rectangular Microstrip Patch Antenna) with the mended ground plane is presented for wide-band applications. In this article, wide bandwidth is achieved by proper loading of slots and notches with improved gain. The measured result proves that the proposed antenna exhibits good impedance matching, VSWR lies below 2 and above 1 in magnitude, high gain and more than 85% of radiation efficiency over the entire frequency band. The simulated and experimented results are validated over the operating frequency range of 2.41 GHz to 9.55 GHz and agree well. From a collective view of radiation patterns, the antenna acts correspondingly to the normal printed monopoles, which is suitable for wide-band applications.

REFERENCES

1. Garg, R., P. Bhartia, I. Behl, and A. Ittipiboon, *Microstrip Antenna Design Handbook*, Artech House Inc., Norwood, MA, 2001.
2. Kumar, G. and K. P. Ray, *Broadband Microstrip Antenna*, Artech House, Boston, 2003.
3. Kumari, K., A. Singh, M. Aneesh, and J. A. Ansari, "Novel design of microstrip antenna with improved bandwidth," *International Journal of Microwave Science and Technology*, Vol. 2014, 1–7, Article ID 659592, Hindawi, 2014.
4. Ansari, J. A., N. P. Yadav, A. Mishra, P. Singh, and B. R. Vishvakarma, "Analysis of multilayer rectangular patch antenna for broadband operation," *Wireless Personal Communications*, Vol. 62, 315–327, Springer, 2012.
5. Ammann, M. J. and Z. N. Chen, "A wide-band shorted planar monopole with bevel," *IEEE Transactions on Antennas and Propagation*, Vol. 51, No. 4, 901–903, 2003.
6. Goswami, S. A. and D. Karia, "A compact monopole antenna for wireless applications with enhanced bandwidth," *International Journal of Electronics and Communications*, Vol. 72, 33–39, Elsevier, 2017.
7. Chiang, K. H. and K. W. Tam, "Microstrip monopole antenna with enhanced bandwidth using defected ground structure," *IEEE Antennas and Wireless Propagation Letters*, Vol. 7, 532–535, 2008.
8. Gopikrishna, M., D. D. Krishna, A. R. Chandran, and C. K. Aanandan, "Square monopole antenna for ultra wide band communication applications," *Journal of Electromagnetic Waves and Applications*, Vol. 21, No. 11, 1525–1537, 2007.
9. Li, Z.-Y., X. S. Zhu, C. Y. Yin, and Y. Huang, "A broadband circularly polarized monopole antenna," *International Journal of RF and Microwave Computer Aided Engineering*, Vol. 29, No. 6, 1–8, Wiley, 2019.
10. Saha, T. K., C. Goodbody, T. Karacolak, and P. K. Sekhar, " A compact monopole antenna for ultra-wideband applications," *Microwave Optical Technology Letters*, Wiley, Vol. 61, No. 1, 182–186, 2019.
11. Boutejdar, A. and W. A. Ellatif, "A novel compact UWB monopole antenna with enhanced bandwidth using triangular defected microstrip Structure and stepped cut technique," *Microwave and Optical Technology Letters*, Vol. 58, No. 6, 1514–1519, Wiley, 2016.
12. Peram, A., A. S. R. Reddy, and M. N. G. Prasad, "Miniaturized single layer Ultra Wide Band (UWB) patch antenna using a partial ground plane," *Wireless Personal Communications*, Springer, 1–17, 2019.
13. Singhal, S. and A. K. Singh, "Asymmetrically CPW-fed hourglass shaped UWB monopole antenna with defected ground plan," *Wireless Personal Communications*, Vol. 94, No. 3, 1685–1699, Springer, 2017.
14. Ojaroudi, N., "Compact UWB monopole antenna with enhanced bandwidth using rotated L-shaped slots and parasitic structures," *Microwave and Optical Technology Letters*, Vol. 56, No. 1, 175–178, Wiley, 2014.

15. Sharma, A., P. Khanna, K. Shinghal, and A. Kumar, "Design of CPW-fed antenna with defected substrate for wideband applications," *Journal of Electrical and Computer Engineering*, Vol. 2016, 1–10, Article ID 6546481, Hindawi, 2016.
16. Gautam, A. K., A. Bisht, and B. K. Kanaujia, "A wideband antenna with defected ground plane for WLAN/WiMAX applications," *International Journal of Electronics and Communications*, Vol. 70, No. 3, 354–358, Elsevier, 2016.
17. Mandal, K. and P. P. Sarkar, "A compact low profile wideband U-shape antenna with slotted circular ground plane," *International Journal of Electronics and Communications*, Vol. 70, No. 3, 336–340, Elsevier, 2016.
18. Baudha, S. and D. K. vishwakarma, "Bandwidth enhancement of a planar monopole microstrip patch antenna," *International Journal of Microwave and Wireless Technologies*, Vol. 8, 1231–1235, Cambridge University Press, 2016.
19. Murugan, N. A., R. Balasubramanian, and H. R. Patnam, "Printed planar monopole antenna design for ultra-wideband communications," *Radio Electronics and Communications Systems*, Vol. 61, No. 6, 267–273, Springer, 2018.
20. Awad, N. M. and M. K. Abdelazeez, "Multislot microstrip antenna for ultra-wide band applications," *Journal of King Saud University-Engineering Sciences*, Vol. 30, 38–45, Elsevier, 2018.
21. Baudha, S. and M. V. Yadav, "A novel design of a planar antenna with modified patch and defective ground plane for ultra-wideband applications," *Microwave and Optical Technology Letters*, Vol. 61, 1320–1327, Wiley, 2019.
22. Huang, Y. and K. Boyle, *Antennas: From Theory to Practice*, Chapter-7 Antenna Manufacturing and Measurements, 272–273, Wiley Publication, 2008.
23. Tang, H., K. Wang, R. Wu, C. Yu, J. Zhang, and X. Wang, "A novel broadband circularly polarized monopole antenna based on C-shaped radiator," *IEEE Antennas and Wireless Propagation Letters*, Vol. 16, 964–967, 2016.
24. Roy, B., S. K. Chowdhury, and A. K. Bhattacharjee, "Symmetrical hexagonal monopole antenna with bandwidth enhancement under UWB operations," *Wireless Personal Communications*, 1–11, Springer US, 2019.
25. Tiwari, R. N., P. Singh, and B. K. Kanaujia, "Asymmetric U-shaped printed monopole antenna embedded with T-shaped strip for bluetooth, WLAN/WiMAX applications," *Wireless Networks*, 1–11, Springer, US, 2018.
26. Okas, P., A. Sharma, G. Das, and R. K. Gangwar, "Elliptical slot loaded partially segmented circular monopole antenna for super wideband application," *International Journal of Electronics and Communications*, Vol. 88, 63–69, Elsevier, 2018.
27. Yang, L., N.-W. Liu, Z.-Y. Zhang, G. Fu, Q.-Q. Liu, and S. Zuo, "A novel single feed omnidirectional circularly polarized antenna with wide AR bandwidth," *Progress In Electromagnetics Research C*, Vol. 51, 35–43, 2014.
28. Chen, L., X. Ren, Y.-Z. Yin, and Z. Wang, "Broadband CPW-fed circularly polarized antenna with an irregular slot for 2.45 GHz RFID reader," *Progress In Electromagnetics Research Letters*, Vol. 41, 77–86, 2013.
29. Valagiannopoulos, C. A., "On smoothening the singular field developed in the vicinity of metallic edges," *International Journal of Applied Electromagnetics and Mechanics*, Vol. 31, No. 2, 67–77, 2009.
30. Valagiannopoulos, C. A., "On examining the influence of a thin dielectric strip posed across the diameter of a penetrable radiating cylinder," *Progress In Electromagnetics Research C*, Vol. 3, 203–214, 2008.
31. Valagiannopoulos, C. A., "On measuring the permittivity tensor of an anisotropic material from the transmission coefficients," *Progress In Electromagnetics Research B*, Vol. 9, 105–116, 2008.